AJNR

Radiation Dose of the Lens in Trans-sphenoidal Pituitary Surgery: Pros and Cons of a Conventional Setup Using Fluoroscopic Guidance and CT-Based Neuronavigation

S. Ulmer, E. Schulz, B. Moeller, U.R. Krause, A. Nabavi, H.M. Mehdorn and O. Jansen

AJNR Am J Neuroradiol 2007, 28 (8) 1559-1564
doi: https://doi.org/10.3174/ajnr.A0588
http://www.ajnr.org/content/28/8/1559

ORIGINAL RESEARCH

Radiation Dose of the Lens in Trans-sphenoidal Pituitary Surgery: Pros and Cons of a Conventional Setup Using Fluoroscopic Guidance and CT-Based Neuronavigation

S. Ulmer
E. Schulz
B. Moeller
U.R. Krause
A. Nabavi
H.M. Mehdorn
O. Jansen

BACKGROUND AND PURPOSE: We determined the radiation dose in patients' lenses during pituitary surgery with either conventional fluoroscopy or CT-guided neuronavigation.

MATERIALS AND METHODS: Thermoluminescent dosimeters (TLD-100H) were attached to the lenses of an anthropomorphic Alderson-Rando head phantom. Simulation of the conventional setup of continuous fluoroscopy (61 kV peak, 2.01 mAs) with collimation and automatic exposure control was used with 1 TLD being removed every 5 seconds, followed by another experiment with 1 being removed every 30 seconds. For CT-guided neuronavigation, a spiral of 3-mm-thick sections without gap was performed (140 kV, 220 mA). Patients' charts ($n = 87$) were reviewed in terms of radiation exposure and perioperative complications.

RESULTS: Radiation dose is distance-dependent ($P < .002$), with an exposure-time-dependent linear increase ($R^2 = 99.27$, $P < .0001$) close to the primary beam only. The radiation dose of the CT (mean, 39.39 mGy) was fivefold higher compared with the maximal time of 3 minutes (8 mGy) reached in our patients by using the conventional setup. CT offers more detailed 3D anatomy available at any time intraoperatively. Tolerance doses needed to develop cataracts were not reached, and perioperative complications occurred without significant differences (Mann-Whitney *U* test, $P = .39$) using either method. Continuous use of fluoroscopy reached the mean value of CT after 14.33 minutes.

CONCLUSION: Neuronavigation provides better anatomic information and avoids repetitive exposure and accumulation to the staff, with the disadvantage of an increased radiation exposure to the patient causing at least no acute harm. Long-term effects are hard to prove but cannot be neglected either.

Knowledge of tolerance doses (TD) of tissue plays an important role, especially in radiation therapy. To estimate dose-related deterioration, Rubin and Cassarett[1] introduced the TD 5/5 and TD 50/5, which reflect the probability of 5% or 50% complication of different tissues within 5 years. Dose-related deterioration of the eye in radiation therapy differs between the lens and retina/optic nerve in relation to the fraction size.[1]

There are studies that deal with the consequences of radiation of the brain; however, less data exist on the consequences of radiation of the orbital tissues. According to the review of Emami et al,[2] which is still routinely used, radiation dose varies among the orbital organs from TD 5/5 of only 10 Gy and TD 50/5 of 18 Gy, respectively, of the lens developing a cataract[3] to TD 5/5 of 45 Gy and TD 50/5 of 65 Gy, respectively, of the retina,[4,5] to TD 5/5 of 50 Gy and TD 50/5 of 65 Gy of the chiasm[6] or optic nerve.[4,7-11] A more recent review resulting from a consensus conference[12] reported lower tolerance thresholds with 16 Gy for the lens (2-Gy/day threshold), 46 Gy for the retina, 30 Gy for the cornea, and 55 Gy for the optic nerve. These thresholds were supported by further case reports.[13,14] Tissue damage is dependent on fraction size and cumulative dose.

Vano et al[15] reported cataract development in interventionalists. The dose exposure in this population could only be estimated retrospectively according to the number of procedures per year and the average time used for the interventions. This report demonstrated the risk of tissue damage caused by radiation exposure in the clinical setting.

Radiation doses of conventional CT scans are usually underestimated by patients, physicians, and even radiologists.[16] Depending on the applied CT protocol, the radiation dose to the lens in cranial CT (CCT) scans was estimated to be 30 mGy, 70 mGy in scanning the sinuses, and up to 130 mGy in trauma imaging.[17] A recent article[18] reported on radiation exposure by repeat CT scanning combined with angiographies in the diagnosis of cranial aneurysms that led to transient hair loss in some cases.

The trans-sphenoidal approach for pituitary surgery was first described by Schloffer in 1907[19] and has been modified several times; however, this surgical approach has remained the gold standard.[20] In healthy adults, the intrasellar space is approximately 1 cm in diameter. With this trans-sphenoidal keyhole approach, abutting anatomic structures such as the internal carotid artery (ICA), cranial nerves, and the cavernous sinus are at a relative risk during the resection of an adenoma. Image guidance, conventionally performed by fluoroscopy, enables intermittent monitoring of the approach and

Received September 22, 2006; accepted after revision January 27, 2007.

From the Section of Neuroradiology (S.U., O.J.), Department of Neurosurgery, and the Departments of Neurology (B.M.) and Neurosurgery (U.R.K., A.N., H.M.M.), University Hospital of Schleswig-Holstein, Kiel, Germany; and the Department of Radiology and Nuclear Medicine (E.S.), University Hospital of Schleswig-Holstein, Luebeck, Germany.

Paper previously presented in part at: European Congress of Radiology, March 4–8, 2005; Vienna, Austria; and the Annual Meeting of the German Neurosurgical Society, May 7–11, 2005; Strasbourg, France.

Please address correspondence to: Stephan Ulmer, MD, Section of Neuroradiology, Department of Neurosurgery, University Hospital of Schleswig-Holstein, Schittenhelmstr 10, 24105 Kiel, Germany; e-mail: ulmer@email.com

DOI 10.3174/ajnr.A0588

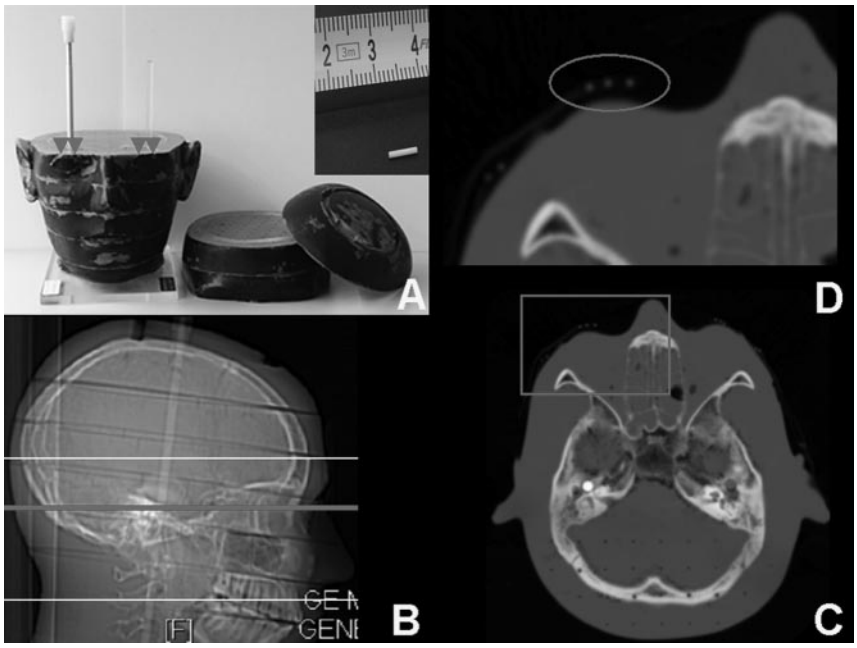

Fig 1. *A,* The anthromorphic Alderson-Rando head phantom consists of 1-inch-thick sections with predrilled holes. The arrowheads mark the locations of the TLDs (size relation demonstrated in the upper right corner, 6 mm long, 1 mm diameter) placed on the lenses of the phantom. *B,* Lateral localizer of the phantom on CT with the plotted image stack covering the maxilla to the frontal bone and reference section (as displayed in *C*) through the orbital cavity. *C,* Axial CCT image of the phantom through the orbital cavity with attached TLD on the topographic site of the lenses and adjacent to it on the temporal bone. The TLDs are well depicted. *D,* Magnification of the box in *C*. The TLDs (*circle*) are depicted on the scan on 2 consecutive sections.

documentation of the dissection at all times. In the conventional intraoperative setup, the patient's head is positioned in a C-array to intermittently monitor the surgical approach and the dissection of the tumor fluoroscopically. The use of collimation reduces radiation dose; however, because of the lateral view during fluoroscopy, the orbit is at least in part exposed to the primary beam. Newer imaging techniques such as CT or MR imaging are used preoperatively and for follow-up examinations because of their high anatomic resolution.

A new technology such as computer-guided neuronavigation systems, first introduced by Kato et al[21] in 1991, enables an operation without intraoperative fluoroscopy by using preoperatively acquired 3D image data. Furthermore, conventional fluoroscopy cannot depict the abutting structures at risk in relation to the lesion. MR imaging compared to CT has the advantage of a high resolution for soft tissue but provides less information about bony structures and vice versa. For CT-based neuronavigation, contrast agent is administered intravenously to enhance the ICA and, to a lesser extent, also the cavernous sinus. Besides the option to visualize soft-tissue structures, CT can also nicely display bony landmarks of the skull base, which are traditionally used for guidance of transsphenoidal pituitary surgery. Intraoperatively, the surgeon can, furthermore, switch between both windows in the neuronavigation device.

Damage of abutting perisellar structures could result in tremendous complications, including major bleeding, dissection of the ICA, stroke, and visual disturbance or complete loss of vision; therefore, the most precise detailed continuously available anatomy is desirable, which can be provided by the use of neuronavigation. After a single use of a CCT, impairment of patients has not been reported, and CCT is regarded as a safe procedure used in daily clinical routine. Harm to the patient after fluoroscopy on the other hand, which is used intraoperatively in a variety of procedures, has also not been reported; however, the issue of applied radiation has not been addressed in either setting for this kind of resection to date. In this study, we, therefore, investigated the dose of radiation found in patients' lenses during pituitary surgery with conventional fluoroscopy or CT-guided neuronavigation.

Methods

All patients gave written informed consent to the study, which was approved by the local institutional review board. We reviewed the charts of the patients who had undergone trans-sphenoidal resection of pituitary tumors with either neuronavigation ($n = 20$) or the conventional setup ($n = 67$) and documented the cumulative fluoroscopy time of intraoperatively performed intermittent fluoroscopy in the latter group. Perioperative complications were weighted according to their clinical severity into a 4-rank scale (from 0 to 3). Rank 0 included no complications and complete resection of the tumor documented on the postoperatively performed MR imaging or CT. Rank 1 included temporary postoperative CSF leakage, diabetes insipidus, and hormonal disturbances without the need for postoperative hormone substitution. Rank 2 included hypocortisolism (Addison disease) with postoperative need for cortisol substitution, incomplete resection, meningitis, and other disturbances of the patients not rated as rank 3. Rank 3 included all kinds of perioperative bleeding, any extended need for intensive care (>24 hours postoperatively), the need for reoperations, or the death of the patient. Furthermore, visual acuity and visual field deficiency were analyzed in a separate manner because the tumor may already have affected vision or have caused visual field defects preoperatively. The changes postoperatively could, therefore, be equal, worse, or improved postoperatively. Because of the groups that were not normally distributed and the different number of patients within the groups, patients undergoing surgery with intraoperative fluoroscopy or neuronavigation were compared with respect to perioperative complications by using a nonparametric Mann-Whitney *U* test for independent samples.

To determine the applied radiation by either fluoroscopy or CT, we used an anthropomorphic Alderson-Rando head phantom (Phantom Laboratory, Salem, NY) simulating intraoperative conditions. This phantom provides an opportunity to place thermoluminescent dosimeters (TLDs) in the head of the phantom at the site of the retina or other intracranial structures as well as on the lens. TLDs were located in coronal orientations (Fig 1). These copper-doped lithium fluoride dosimeters (TLD-100H; LiF:Mg, Cu, P) absorb high-energy photons during fluoroscopy.

To simulate the conventional setup in the operating room, we overextended the phantom and placed it into the head holder on the operating table between the x-ray tube and image intensifier of the mobile C-arm array (BV 300; Philips, Best, the Netherlands). The unit

Table 1: Comparison of radiation dose values acquired from TLDs distal or proximal to the primary beam (fluoroscopy)

Time (s)	Radiation Dose$_{proximal}$ (μGy)	Radiation Dose$_{distal}$ (μGy)
5	0.33	0.07
10	0.33	0.1
15	0.49	0.08
20	0.71	0.07
25	1.07	0.08
30	1.17	0.07
35	1.43	–
40	1.72	0.12
45	1.98	0.20
50	2.31	0.29

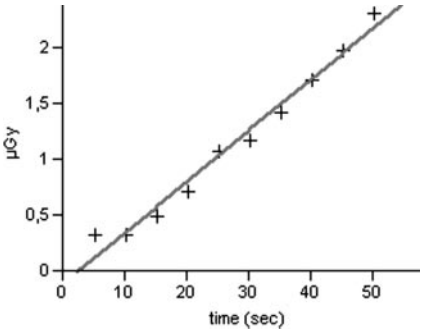

Fig 2. Radiation dose plotted against time course. There is a linear time-dependent increase of the radiation dose close to the primary beam ($R^2 = 99.27$, $P < .0001$).

is a single-plane multidirectional fluoroscope providing the ability of last-image hold. The focus-to-image-intensifier distance is 100 cm, leading to a focus-to-phantom distance of approximately 80 cm. On the basis of our clinical experience in the use of intraoperative fluoroscopy, we performed 2 different experiments. In the first experiment, we placed 10 TLDs (TLD-100H) on the lenses of the phantom on both sides (close and distal to the primary beam). Two separate runs were performed. Continuous fluoroscopy mode was used with automatic exposure control (Philips BV 300; 61 kilovolt peak, 2.01 mAs), collimation, and zooming on the sella and automatic brightness control to see only the necessary bony structures of the maxilla and sella during the simulated debulking of the lesion. Every 5 seconds, 1 TLD was removed on alternating sides, leading to consecutive values of both sides to depict dose changes after the first minute of cumulative fluoroscopy. Values of the TLDs were compared by using a Student paired *t* test.

After this setup, another experiment was performed with 30 TLDs placed on the temporal bone and lens close to the primary beam; 1 TLD was removed every 30 seconds.

Even though intermittent fluoroscopy is used intraoperatively, the fluoroscopy unit counts and adds the overall fluoroscopy time and radiation applied during the entire procedure. Both experiments were, therefore, designed to cover different cumulative fluoroscopy times. Time-dependent changes were analyzed by using a cross-correlation.

In CT-guided neuronavigation, usually 7 fiducial markers are attached to the subject's maxilla and forehead to allow an intraoperative image-to-patient registration. The patient's head is placed in a supine position. The image stack, consisting of a spiral of sections of 3-mm thickness without gap (pitch 1), is performed on a conventional clinical scanner (140 kV, 220 mAs; HiSpeed Advantage; GE Healthcare, Milwaukee, Wis) covering the maxillary bone up to the frontal bone, including the entire orbital cavity. Contrast agent is injected intravenously to enhance the ICA, the cavernous sinus, and other peri- and intrasellar soft tissues. Beside soft-tissue structures, CCT also scans all bony structures of the skull base at the same time without need for another examination. This process enables the neurosurgeon intraoperatively to switch between the soft-tissue and bone window at any time. Usually, these data are transferred via Ethernet into the navigation computer in the operating room. For this experiment, the TLDs were placed on the lenses of the phantoms, which, due to their size (6-mm length, 1-mm diameter) and their coronal orientation, were displayed on 2 consecutive CT sections.

The chosen settings for either fluoroscopy or CT represent our clinical settings for pituitary surgery.

Analysis of the TLDs was performed by using the Harshaw TLD Reader (Model 5500, Thermo Scientific, Waltham, Mass). After being exposed to radiation, the lithium fluoride crystals of the TLDs re-emit photons (wavelengths) when heated during the readout process. The amount of photons and thus the intensity of light of the re-emitted photons are proportional to the amount of energy absorbed during fluoroscopy, which is recorded and measured quantitatively (as charge values in nanocoulombs). Previously, a conversion factor was calculated for each TLD on the basis of the results of a simultaneous measurement by using a standard dosimeter (Diadose; PTW, Freiburg, Germany) and all TLDs during parallel exposure of defined radiation on a fluoroscopy table (Ultimax, MDX-8000A; Toshiba, Tokyo, Japan). Using this conversion factor, we could calculate the real radiation dose achieved during the experiments.

To compare values of the TLDs in the conventional setting and in the neuronavigation setup, we performed a Student paired *t* test. A *P* value of .05 was regarded as significant.

Results

As demonstrated in Table 1, the dose of the TLDs close to the radiation beam was above those levels reached by the TLDs distal to the primary beam (paired *t* test, $P < .002$), demonstrating the known fact that radiation exposure is distance-dependent. The TLDs close to the primary beam demonstrated an exposure-time-dependent linear increase (Fig 2, $R^2 = 99.27$, $P < .0001$).

The radiation dose of the neuronavigation CT (mean, 39.39 mGy; range, 36.68–41.49 mGy) was far above the values reached after 1 minute of continuous fluoroscopy in the operating room setting as well as above the dose that was reached after a cumulative fluoroscopy time of 3 minutes (8 mGy), which was never exceeded in the fluoroscopically guided patient group (paired *t* test, $P < .001$).

In continuous fluoroscopy, with 1 TLD being removed every 30 seconds from the skin surface close to the radiation beam, we found a linear exposure-time-dependent increase in radiation dose ($R^2 = 99.54$, $P < .0001$) that reached the mean value of that of the CT exposure after approximately 14 minutes 20 seconds (Fig 3 and Table 2).

In our patient group, fluoroscopy times intraoperatively ranged from 6 seconds to 2 minutes 47 seconds, with a mean time of 47 seconds (SD, 41 seconds). In both groups, perioperative complications occurred. In the fluoroscopically guided group, minor complications (rank 1) occurred 7 times, mediocre complications (rank 2) occurred 5 times, and severe complications (rank 3) occurred 5 times. In the neuronavigationally guided

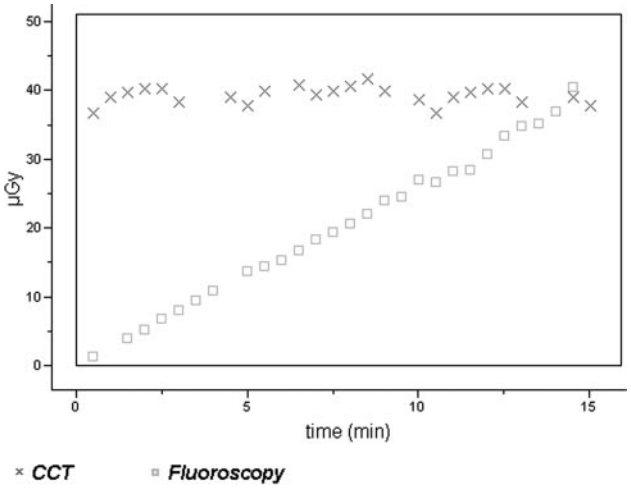

Fig 3. Radiation dose plotted against time course with continuous fluoroscopy (*squares*) and CCT (*crosses*). Both lines cross after 14 minutes 20 seconds.

Table 2: Comparison of radiation dose acquired from TLDs in fluoroscopy or CCT

Time (s)	Radiation $Dose_{fluoroscopy}$ (μGy)	Radiation $Dose_{CCT}$ (μGy)
30	1.35	36.68
60	–	38.83
90	3.92	39.69
120	5.24	40.09
180	6.83	40.06
210	8.05	38.23
240	9.55	–
270	10.95	–
300	–	38.82
330	13.82	37.65
360	14.51	39.82
390	15.41	–
420	16.69	40.59
450	18.36	39.34
480	19.33	39.86
510	20.56	40.56
540	22.02	41.49
570	24.05	39.87
600	24.56	–
630	27.09	38.61
660	26.65	36.68
690	28.23	38.83
720	28.52	39.69
750	30.66	40.09
780	33.35	40.06
810	34.75	38.23
840	35.12	–
870	37.04	38.82
900	40.58	37.65

Note:—Values from the CCT are from a single examination, reflect the individual TLDs, and are, therefore, dependent on neither the time nor accumulation. The time column is for the fluoroscopy only.

group, minor complications (rank 1) occurred in one case, mediocre complications (rank 2) occurred in 4 cases, and severe complications (rank 3) occurred in 2 cases. Both groups did not differ significantly (Mann-Whitney *U* test, $P = .33$). Complications in the patient group using intraoperative fluoroscopy were not related to the duration of the cumulative applied fluoroscopy.

Discussion

The radiation dose is distance-dependent. In both settings, the radiation dose was far below the tolerance doses needed to develop cataracts in the follow-up period, estimated as 10 Gy[3] or 16 Gy at TD 5/50[12] with a threshold of 2 Gy per day.[13,14]

Recently, Thomton et al[22] have demonstrated that the multidetector row CT scanner showed a higher in-plane radiation dose and a higher dose in the plane adjacent to the imaged plane, and they concluded that there was a need for modification in scanning protocols due the wide availability of multidetector row scanners. In our series, we determined the in-plane radiation dose and also the radiation dose caused by scatter radiation in both setups. A further attempt should be to lower the radiation dose using CT while keeping the required image quality needed for neuronavigation, applying the ALARA principle (As Low As Reasonably Achievable). Optimizing the setup for fluoroscopy could also reduce the radiation applied intraoperatively; however, the purpose of this study was to compare radiation doses of 2 different image-guided systems used on a daily basis clinically and intraoperatively.

According to our review of the literature, the issue of radiation exposure in this kind of operation has previously not, to our knowledge, been addressed. There are no data of standard durations of intraoperatively applied fluoroscopy to monitor this kind of approach, which turned out to be case-dependent in our series. Even though radiation was several times higher in the CT-guided setup, CT offers more detailed anatomic information than a 2D plane projection fluoroscopy. Tissues at relative risk, such as the ICA and cavernous sinus, can clearly be depicted in relation to the intrasellar lesion and bony landmarks. Image guidance based on neuronavigation displays this information at any time during the resection. With the neuronavigation, the applied radiation dose was still far below tolerance doses considered to cause harm to the patient; therefore, it may be used safely in pituitary surgery. Although this was not the primary focus of this study, the neuronavigation setup offers another advantage that has to be considered. Aside from the fact that a single exposure of low-dose radiation is applied to the patient, when a preoperative navigation dataset is used, the surgeon would not be exposed to repetitive radiation intraoperatively. It should be noted that repetitive radiation exposure to the surgeon accumulates with time, which could result in long-term side effects and complications.[15] As demonstrated, radiation doses in clinical settings are underestimated by patients, physicians, and even radiologists.[16] Physicians such as radiologists are exposed to higher doses than other professions. During the past decades, with reduced exposure and higher protection, there has been no evidence of increased cancer mortality in radiologists, considering that the population of radiologists had significantly increased before 1954.[23]

The clinical impact and health risks of these applied radiation doses remains to be seen. Most recently, the Committee on the Biological Effects of Ionizing Radiation published the new BEIR VII phase 2 report with extensive review of the current literature of low linear energy transfer (LET) radiation.[24] Various aspects have been discussed, including in vitro studies on DNA damage, long-term follow-up on atomic bomb survivors, estimation of cancer risks and long-term follow-up on

patients who had undergone radiation for both malignant or benign disease, as well as applied radiation for diagnostic purposes in children and adults. The probability that low LET radiation will interact with a DNA molecule is low but possible,[25] leading to cell lethality, impaired cell function, or damage involved in the carcinogenic process. Irradiation of blood with doses as low as 0.2 Gy by using x-rays demonstrated dose-response curves of chromosomal aberrations.[26] In all published experimental studies with rodents, it was difficult or impossible to determine excess tumor rates at doses substantially less than 1 Gy.[24] Factors such as variations in radiosensitivity during the cell cycle; induction of an adaptive response to an initial exposure, which can reduce the effect of later exposures; bystander effect; induction of persistent genomic instability; and hyper-radiation sensitivity may already be caused by low LET radiation. At low doses, the risk of radiation-induced cancer is independent of the time during which exposure occurs and is an accumulative function of dose.[24]

In the applied dose range of this study, the induction of cancer is very unlikely; however, an effect induced by an acute dose of low LET radiation has a linear quadratic dose-response relationship. In humans, radiation treatment for benign disease demonstrated carcinogenicity of low LET radiation in children treated for tinea capitis with only 1.5-Gy average dose. An increase in meningiomas, gliomas, and nerve sheet tumors compared with age-matched controls in the follow-up period was found.[27,28] Although clinical proof of the health risks due to diagnostic x-ray use is hard to find, it cannot be neglected. Cumulative risks of inducing cancer by diagnostic imaging were estimated in relation to the frequency of diagnostic x-ray use in 15 industrial countries. In Japan, diagnostic x-ray use may cause 3.2% of the cumulative risk of inducing cancer to age 75 years, equivalent to 7587 cases of cancer attributable to diagnostic x-ray per year. Japan had the highest annual x-ray frequency per 1000 population, followed by Germany and the United States. For the United States, 0.9% of cancers or 5695 cases of cancer per year could be caused by diagnostic x-rays.[29]

In our study, there was no statistically significant difference in perioperative complications in either group. This may be due to the experience of the surgeon in this type of operation, with reduced need for fluoroscopy as well as his familiarity with the use of neuronavigation guidance. Through its wide availability and use in other types of resection, neuronavigation is thought to be extremely helpful and would benefit less experienced surgeons. The issue of complications by using either neuronavigation or fluoroscopy intraoperatively has previously not been addressed; however, new technologies must prove to be at least adequate if not better than the gold standard, which was demonstrated in this study.

Brain shift in trans-sphenoidal pituitary surgery is usually negligible; however, with large space-occupying and displacing lesions, an update intraoperatively after debulking may be required.[30] The use of a nonionization technique such as MR imaging seems to be reasonable in this perspective because the patient and surgeon would not be exposed to radiation. Advances in the technique also enable trans-sphenoidal surgery by using MR imaging-guided neuronavigation with the option of intraoperative updates by using a high-field MR imaging scanner[31]; however, these techniques remain restricted to a few specialized centers worldwide.[31-33] With advances in MR imaging and its availability, neuronavigation can also be based on these preoperatively acquired images, having both advantages, no radiation and high-resolution images with detailed anatomic information.

Conclusion

We have demonstrated that even though the use of CT-guided neuronavigation resulted in higher radiation exposure to the patient compared with a conventional setup with intraoperative fluoroscopy, the dose was far below a threshold considered to cause harm to the patient. Detailed 3D anatomic information during the resection of a pituitary lesion is the greatest advantage of the use of neuronavigation and avoids repetitive exposure to the surgeon and operating room staff. A change to MR imaging as the preoperative imaging modality for neuronavigation will furthermore avoid radiation to the patient. Additionally MR imaging will provide an even more detailed high-resolution 3D anatomic dataset. Responsible use of clinical radiation results in reasonable radiation exposure to the patient.

References

1. Rubin P, Cassarett GW, eds. *Clinical Radiation Pathology.* Vol II. Philadelphia: WB Saunders; 1968
2. Emami B, Lyman J, Brown A, et al. **Tolerance of normal tissue to therapeutic irradiation.** *Int J Radiat Oncol Biol Phys* 1991;21:109–22
3. Deeg HJ, Flournoy N, Sullivan KM, et al. **Cataracts after total body irradiation and marrow transplantation: a sparing effect of dose fractionation.** *Int J Radiat Oncol Biol Phys* 1984;10:957–64
4. Shukovsky LJ, Fletcher GH. **Retinal and optic nerve complications in a high-dose irradiation technique of ethmoid sinus and nasal cavity.** *Radiology* 1972;104:629–34
5. Nakissa N, Rubin P, Strohl R, et al. **Ocular and orbital complications following radiation therapy of paranasal sinus malignancies and review of literature.** *Cancer* 1983;51:980–86
6. Hammer HM. **Optic chiasmal radionecrosis.** *Trans Ophthalmol Soc U K* 1983; 103(pt 2):208–11
7. Parsons JT, Bova FJ, Mendenhall WM, et al. **Response of the normal eye to high dose radiotherapy.** *Oncology (Williston Park)* 1996;10:837–47, discussion 847–48, 851–52
8. Brown GC, Shields JA, Sanborn G, et al. **Radiation optic neuropathy.** *Ophthalmology* 1982;89:1489–93
9. Kline LB, Kim JY, Ceballos R. **Radiation optic neuropathy.** *Ophthalmology* 1985;92:1118–26
10. Aristizabal SA, Boone ML, Laguna JF. **Endocrine factors influencing radiation injury to central nervous tissue.** *Int J Radiat Oncol Biol Phys* 1979;5:349–53
11. Pezner RD, Archambeau JO. **Brain tolerance unit: a method to estimate risk of radiation brain injury for various dose schedules.** *Int J Radiat Oncol Biol Phys* 1981;7:397–402
12. Gordon KB, Char DH, Sagerman RH. **Late effects of radiation on the eye and ocular adnexa.** *Int J Radiat Oncol Biol Phys* 1995;31:1123–39
13. Garrott H, O'Day J. **Optic neuropathy secondary to radiotherapy for nasal melanoma.** *Clin Experiment Ophthalmol* 2004;32:330–33
14. Danesh-Meyer HV, Savino PJ, Sergott RC. **Visual loss despite anticoagulation in radiation-induced optic neuropathy.** *Clin Experiment Ophthalmol* 2004;32:333–35
15. Vano E, Gonzalez L, Beneytez F, et al. **Lens injuries induced by occupational exposure in non-optimized interventional radiology laboratories.** *Br J Radiol* 1998;71:728–33
16. Lee CI, Haims AH, Monico EP, et al. **Diagnostic CT scans: assessment of patient, physician, and radiologist awareness of radiation dose and possible risks.** *Radiology* 2004;231:393–98
17. Rehani MM, Berry M. **Radiation doses in computed tomography: the increasing doses of radiation need to be controlled.** *BMJ* 2000;320:593–94
18. Imanishi Y, Fukui A, Niimi H, et al. **Radiation-induced temporary hair loss as a radiation damage only occurring in patients who had the combination of MDCT and DSA.** *Eur Radiol* 2005;15:41–46
19. Welbourn RB. **The evolution of transsphenoidal pituitary microsurgery.** *Surgery* 1986;100:1185–90
20. Grunert P, Darabi K, Espinosa J, et al. **Computer-aided navigation in neurosurgery.** *Neurosurg Rev* 2003;26:73–99, discussion 100–01

21. Kato A, Yoshimine T, Hayakawa T, et al. **A frameless, armless navigational system for computer-assisted neurosurgery: technical note.** *J Neurosurg* 1991;74:845–49
22. Thomton FJ, Paulson EK, Yoshizumi TT, et al. **Single versus multi-detector row CT: comparison of radiation doses and dose profiles.** *Acad Radiol* 2003;10:379–85
23. Berrington A, Darby SC, Weiss HA, et al. **100 years of observation on British radiologists: mortality from cancer and other causes 1897–1997.** *Br J Radiol* 2001;74:507–19
24. Committee on the Biological Effects of Ionizing Radiation. *Health Risks From Exposure to Low Levels of Ionizing Radiation: BEIR VII phase 2*. Washington, DC: The National Academy of Science; 2006
25. Nikjoo H, Bolton CE, Watanabe R, et al. **Modelling of DNA damage induced by energetic electrons (100 eV to 100 keV).** *Radiat Prot Dosimetry* 2002;99:77–80
26. Knehr S, Huber R, Braselmann H, et al. **Multicolour FISH painting for the analysis of chromosomal aberrations induced by 220 kV X-rays and fission neutrons.** *Int J Radiat Biol* 1999;75:407–18
27. Sadetzki S, Chetrit A, Freedman L, et al. **Long-term follow-up for brain tumor development after childhood exposure to ionizing radiation for tinea capitis.** *Radiat Res* 2005;163:424–32
28. Ron E, Modan B, Boice JD Jr, et al. **Tumors of the brain and nervous system after radiotherapy in childhood.** *N Engl J Med* 1988;319:1033–39
29. Berrington de Gonzalez A, Darby S. **Risk of cancer from diagnostic X-rays: estimates for the UK and 14 other countries.** *Lancet* 2004;363:345–51
30. Nabavi A, Black PM, Gering DT, et al. **Serial intraoperative magnetic resonance imaging of brain shift.** *Neurosurgery* 2001;48:787–97, discussion 797–98
31. Fahlbusch R, Keller B, Ganslandt O, et al. **Transsphenoidal surgery in acromegaly investigated by intraoperative high-field magnetic resonance imaging.** *Eur J Endocrinol* 2005;153:239–48
32. Nimsky C, Ganslandt O, Cerny S, et al. **Quantification of, visualization of, and compensation for brain shift using intraoperative magnetic resonance imaging.** *Neurosurgery* 2000;47:1070–79, discussion 1079–80
33. Pergolizzi RS Jr, Nabavi A, Schwartz RB, et al. **Intra-operative MR guidance during trans-sphenoidal pituitary resection: preliminary results.** *J Magn Reson Imaging* 2001;13:136–41